Observed Changes in Daily Precipitation Intensity in the United States

Ryan D. Harp[1,1] and Daniel E Horton[2,2]

[1]Institute for Sustainability and Energy at Northwestern; Northwestern University
[2]Northwestern University

May 17, 2023

Abstract

The characterization of changes over the full distribution of precipitation intensities remains an overlooked and underexplored subject, despite their critical importance to hazard assessments and water resource management. Here, we aggregate daily in situ Global Historical Climatology Network precipitation observations within seventeen internally consistent domains in the United States for two time periods (1951-1980 and 1991-2020). We find statistically significant changes in wet day precipitation distributions in all domains – changes primarily driven by a shift from lower to higher wet day intensities. Patterns of robust change are geographically consistent, with increases in the mean (4.5-5.7%) and standard deviation (4.4-8.7%) of wet day intensity in the eastern U.S., but mixed signals in the western U.S. Beyond their critical importance to the aforementioned impact assessments, these observational results can also inform climate model performance evaluations.

Observed Changes in Daily Precipitation Intensity in the United States

Ryan D. Harp[1, 2], Daniel E. Horton[1, 2]

[1]Institute for Sustainability and Energy at Northwestern, Northwestern University, Evanston, IL

[2]Department of Earth and Planetary Sciences, Northwestern University, Evanston, IL

Resubmitted to Geophysical Research Letters

19 July, 2022

Key Points

- We find consistent shifts from lower to higher daily precipitation intensities, particularly in the central and eastern United States
- All contiguous United States domains show significant changes in their distributions of precipitation intensity from 1951-1980 to 1991-2020
- Mean and standard deviation of wet day precipitation intensities increase for nearly all domains in the central and eastern United States

Abstract

The characterization of changes over the full distribution of precipitation intensities remains an overlooked and underexplored subject, despite their critical importance to hazard assessments and water resource management. Here, we aggregate daily *in situ* Global Historical Climatology Network precipitation observations within seventeen internally consistent domains in the United States for two time periods (1951-1980 and 1991-2020). We find statistically significant changes in wet day precipitation distributions in all domains – changes primarily driven by a shift from lower to higher wet day intensities. Patterns of robust change are geographically consistent, with increases in the mean (4.5-5.7%) and standard deviation (4.4-8.7%) of wet day intensity in the eastern U.S., but mixed signals in the western U.S. Beyond their critical importance to the aforementioned impact assessments, these observational results can also inform climate model performance evaluations.

Plain Language Summary

Lots of research has been done to see how precipitation event totals are affected by climate change. Instead of yearly totals or extreme precipitation, we look at how daily precipitation is changing at all intensities, which has effects on natural hazards and related risks. We group daily rain gauge measurements within seventeen climate regions in the United States for two thirty-year time periods: 1951-1980 and 1991-2020. We find changes in daily precipitation

intensity in all regions, changes that are mostly caused by a shift from lower to higher intensity events. We also identify a broad area within the central and eastern U.S. with consistent increases in average precipitation and its variability. Changes are mixed in the western U.S. In addition to the impacts mentioned above, our results can also be used to see how well climate models perform.

Keywords

daily precipitation, precipitation variability, precipitation intensity distribution, GHCN, NEON, NCA

1. Introduction

Anthropogenic climate change is driving shifts in global precipitation patterns (Douville et al., 2021). Recent studies have characterized these shifts across a diversity of metrics and scales, including annual totals, frequencies of occurrence, and zonal distributions. At the daily scale, recent efforts have demonstrated robust changes in extreme precipitation intensities (i.e., the 95th percentile and above; Seneviratne et al., 2021). However, characterization of changes in the full distribution of precipitation intensities – events which are, by definition, much more common – are often overlooked. While extreme precipitation events can produce outsized

67 damages given their exceptional nature, changes in non-extreme precipitation have critical
68 impacts on many Earth systems, including agriculture (Shortridge, 2019), infrastructure (Cook
69 et al., 2019), and natural hazards (Dinis et al., 2021; Cannon et al., 2008). For example, including
70 increasing daily precipitation variability in projections of future crop yields resulted in a 2-6%
71 reduction in relative yields compared to projections excluding this factor (Shortridge, 2019).
72 Here, to more comprehensively characterize daily precipitation shifts, we explore changes in the
73 full distribution of wet day precipitation intensities over seventeen climatically-distinct regions
74 across the United States.
75
76 *1.1. Why is precipitation changing?*
77 Globally, mean annual precipitation is expected to increase ~2%/K with warming (Trenberth,
78 2003; Held and Soden, 2006; Wentz et al., 2007; Wood et al., 2021), though considerable
79 observed and projected spatiotemporal variability underlie this estimate (e.g., Polade et al.
80 (2014) globally; Caloiero et al. (2018) in Europe). Anthropogenic climate change is expected to
81 alter precipitation patterns via both thermodynamic and dynamic processes. Thermodynamic
82 changes are driven by an increase in atmospheric moisture content with warming, which occurs
83 at a rate of ~6-7%/K as described by the Clausius-Clapeyron relationship. An increase in
84 atmospheric moisture content leads to an increase in globally averaged rainfall, though
85 magnitude estimates of the corresponding increase depend on spatial and temporal scales
86 (Westra et al., 2014; Cannon and Innocenti, 2019; Sun et al., 2021; Wood and Ludwig, 2020;
87 Wood et al., 2021; Bador et al., 2018, Giorgi et al., 2019). Globally averaged precipitation
88 increases are also constrained by Earth's energy budget, which leads to a discrepancy between

increased moisture availability and precipitation change (Pendergrass and Hartmann, 2014a). Dynamically-driven precipitation changes are mostly associated with shifts in atmospheric circulation (e.g., Swain et al, 2016; Endo and Kitoh, 2014). Examples of these mechanisms include climatological shifts in cyclone and anticyclone tracks, baroclinic zones, and jets – which are driven by the reduction in the equator-pole temperature gradient – a poleward expansion of the descending branch of Hadley cells, and increases in land-sea temperature gradients (Polade et al., 2014). Altered precipitation totals can also be caused by more subtle changes, such as reductions in storm speeds (Kahraman et al., 2021). The relative importance of these factors varies widely depending on location.

Locally, the rate of increase of precipitation for smaller-scale and heavy precipitation events parallels and can even exceed Clausius-Clapeyron scaling, particularly during convective precipitation (Lenderink and van Meijgaard, 2008; Guerreiro et al., 2018; Risser and Wehner, 2017) or where local conditions shift from favoring stratiform to convective precipitation (Berg and Haerter, 2013; Berg et al., 2013; Ivancic and Shaw, 2016). Prein et al. (2017) project increases in extreme precipitation frequency and intensity with rising temperatures in moist, energy-limited environments, along with abrupt decreases in dry, moisture-limited environments. However, the precise scaling of extreme precipitation to rising temperatures and moisture availability is dependent on a multitude of factors, including characteristics of local convection, topography, and synoptic-scale dynamics (Moustakis et al., 2020).

1.2 How is daily precipitation variability changing?

Increases in the frequency and intensity of extreme daily precipitation have been widely observed (Westra et al., 2014; Donat et al., 2016; Asadieh and Krakauer, 2015; Sun et al., 2021; Wood et al., 2021; Alexander et al., 2006; Myhre et al., 2019) and generally agree with increases projected by climate model simulations (Moustakis et al., 2021; Toreti et al., 2013; Groisman et al., 2005; Fischer and Knutti, 2014; Fischer and Knutti, 2016; Myrhe et al., 2019; Min et al., 2011; O'Gorman, 2015). For example, Lehmann et al. (2015) found that record-breaking rainfall events occurred 12% more often than expected globally from 1981-2010 with an estimated 26% chance that a record-setting rainfall event is due to long-term climate change. Min et al. (2011) examined observed and modeled changes and found that climate change has contributed to the observed intensification of heavy precipitation events over two-thirds of the Northern Hemisphere. Sub-daily extreme precipitation is both observed and projected to increase at an even faster rate than daily extremes at regional and global scales (e.g., U.S., Prein et al., 2017; Netherlands, Lenderink and van Meijgaard, 2008; global, Westra et al., 2014).

Despite widespread research into precipitation extremes, changes over the full distribution of precipitation intensities are less well-characterized. For instance, Chou et al. (2012) find an increase in heavy precipitation events relative to light in the global tropics in model simulations. Giorgi et al. (2019) find similar results over extratropical land, including an overall reduction in lower intensity event frequency and increase in higher intensity event frequency. Hennessy et al. (1997) modeled changes in daily precipitation and found distribution shifts from low to high intensity at high latitudes along with increased heavier precipitation events coincident with a reduction of moderate events in the mid-latitudes. Despite the

identification of changes in distributions of precipitation intensity at broad global or zonal scales, studies at regional and local scales are sparse.

In the United States, increases in mean annual precipitation and extreme precipitation have been noted, though changes are non-uniform and have seasonal dependencies (Easterling et al., 2017; Goble et al., 2020). Here, we focus on observed changes in daily precipitation. Increases in heavy to extreme precipitation are well established in the central and eastern U.S. (Groisman et al., 2012; Sun et al., 2021; Kunkel et al., 2013; Guilbert et al., 2015; Karl and Knight, 1998; Pryor et al., 2008; Groisman et al., 2001; Villarini et al., 2013; Contractor et al., 2021; Groisman et al., 2005). In addition, increases in light-to-moderate precipitation frequency are driving a general increase in precipitation frequency in the U.S. (Pal et al., 2013; Goodwell and Kumar, 2019; Karl and Knight, 1998; Roque-Malo and Kumar, 2017). However, the evolution of the proportion of lower vs higher intensity wet days is less resolved with contradictory findings reported. For example, Groisman et al. (2012) found more frequent higher intensity events over the central U.S. despite no change in moderate intensity events. In contrast, Karl and Knight (1998) identified an increasing frequency of events across most percentiles and U.S. regions, including an increase in moderate intensity events. While findings focused on the eastern and central U.S. are generally consistent, studies focused on the western U.S. disagree. For example, Contractor et al. (2021) and Higgins and Kousky (2013) find generally increasing frequency and intensity of wet day events over the majority of the U.S. but decreasing moderate to heavy intensity events along the Pacific coast. Their findings are inconsistent with findings of increasing or insignificant extreme precipitation change on the U.S. west coast by Kunkel et al. (2013). Many previous analyses used gridded precipitation products (e.g., Contractor et al.,

2021) that possess known inconsistencies across products (Alexander et al., 2020) and center on heavy-to-extreme precipitation or arbitrary light or moderate thresholds (e.g., 50th percentile or 10mm; Higgins and Kousky, 2013; Kunkel et al., 2013). To overcome these methodological limitations and reconcile disparate findings, here we examine changes over the complete distribution of precipitation intensities by spatially aggregating a large number of *in-situ* station observations across a high number of empirically determined, distinct U.S. climate regions.

2. Methods

To partition the U.S. into climatologically-distinct regions, we adopt the National Ecological Observatory Network (NEON) domains. These twenty domains were designed to be climatically homogeneous within-domains but distinct across-domains and were created using a multivariate geographic clustering analysis incorporating nine different temperature and precipitation variables (National Ecological Observatory Network, n.d.; Schimel, 2011; Keller et al., 2008). We center our analysis on the seventeen domains that compose the contiguous United States (Figure 1). Rather than analyze station records individually, we employ spatial aggregation to provide a larger sample size and better view of change over time given the inherent limitations of individual station statistics and internal climate variability. Spatial aggregation has frequently been employed in precipitation analyses (e.g., Fischer et al., 2013; Groisman et al., 2005; Kunkel et al., 2013). In addition to the seventeen domains within the contiguous U.S., we include findings for the remaining three domains, as well as replicate our

analysis for the U.S. National Climate Assessment regions (NCA; Easterling et al., 2017), in the Supporting Information.

Our analysis uses daily *in-situ* observations of precipitation from the Global Historical Climatology Network Daily (GHCN-D). The GHCN-D database is compiled by NOAA's National Centers for Environmental Information and consists of records from over 80,000 stations and 180 countries and territories, including the most complete collection of daily U.S. data available (Menne et al., 2012). Observations in GHCN-D have a sensitivity of 0.1 mm and undergo a series of nineteen quality control tests to flag duplicate data, climatological outliers, and other inconsistencies, as detailed in Durre et al. (2010).

To examine changes in the distribution of wet day precipitation intensities, we aggregate all wet day precipitation observations for all qualifying stations within each domain, where a wet day is defined as a station-day observing 1 mm or more of precipitation. This is done for two thirty-year periods: 1951-1980 and 1991-2020. We choose the early time period (1951-1980) due to the proliferation of GHCN-D stations that peaked in this interval (see Fig. 3b; Menne et al., 2012); we selected the late time period (1991-2020) as the most recent 30-year interval with available data. The distributions are built around 30-year periods of reference to overcome known impacts of interannual modes of climate variability (e.g., Groisman et al., 2012) and align with World Meteorological Organization guidelines (World Meteorological Organization, 2017). To ensure quality of record and consistency in stations across periods, we include data from a station if 90% of the station-years in both periods are complete, where a complete year is defined as containing 90% or more of all available daily records after removal of any flagged entries. Applying this filter reduces available records from an initial 63,571 to 1,742 that are

suitable for our analysis. Figure 1 depicts station locations and stations per domain. Finally, we manually check extreme outliers against historical records (e.g.., state records, U.S. National Weather Service records), to corroborate their validity. This final check identified 32 unverifiable records that we remove from our analysis (Table S1).

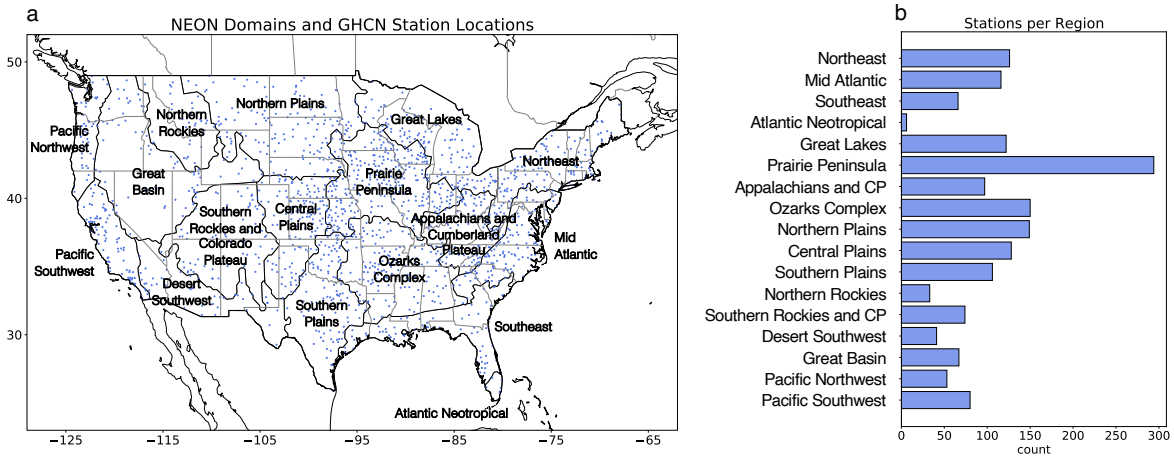

Figure 1: Station Locations and Domain Station Counts. (a) Map of qualifying GHCN-D stations (blue dots) overlaid on the United States with NEON domain boundaries in thick black and state borders in thin grey. (b) Histogram of the number of qualifying stations within each NEON domain.

Qualifying wet day observations are aggregated into early or late period daily precipitation intensity probability distributions via block bootstrapping. Raw observations from qualifying stations are parsed into two-year station-segments, resampled with replacement, and combined. The resultant two-year aggregations are then stacked to produce a single 30-year precipitation intensity distribution sample for each domain; this process is replicated 1,000 times for each period in each domain. We then calculate differences between early and late period distributions across four statistical moments (mean, standard deviation, skew, kurtosis).

This process is replicated for each bootstrap resample to determine statistical confidence intervals for changes in statistical moments. In addition, we characterize changes in the full precipitation intensity distributions by quantifying changes in the number of wet day events within each five percentile increment bin (e.g., 50th-55th percentile), where percentile bin ranges are determined by values in the early period distribution sample.

Finally, the initial early and late precipitation intensity distributions are directly compared through two-sample Kolmogorov-Smirnov and Anderson-Darling tests, both of which are suitable for nonparametric analysis and are insensitive to the number of events in the distributions (Chakravarti et al., 1967; Stephens, 1974). These tests were performed on all available station data within a domain (i.e., not bootstrapped). We employed the Anderson-Darling test in addition to the more common Kolmogorov-Smirnov due to its higher sensitivity to extreme values, though results proved largely consistent. While both tests can determine if distributions are distinct, they do not provide descriptive information as to how the distributions differ. We thus characterize early and late period distribution differences by computing differences in wet day intensity distributions and their statistical moments. However, it should be noted that statistical moments do not comprehensively characterize a distribution. As such, statistically significant changes identified by the Kolmogorov-Smirnov and Anderson-Darling two-sample tests, may not be discernible via the moment difference analysis.

3. Results

Early and late period distributions of wet day precipitation intensity are statistically significantly different ($p < 0.05$) for all NEON domains in the contiguous U.S. (Table S2), with broadly consistent changes observed across central and eastern domains. Specifically, mean wet day precipitation increases in all domains east of the Rocky Mountains (Figure 2a-b) except for one (Atlantic Neotropical), with an intensification in mean wet day precipitation between 4.5-5.7% for the majority of these eastern domains (Figure 2b). Similarly, the standard deviation of wet day precipitation intensity increased between 4.4-8.7% for each eastern domain (Figure 2c) outside of the Atlantic Neotropical. Changes in mean and standard deviation for western domains are mixed in sign and not statistically significant. Table S2 shows the differences in mean, standard deviation, skew, and kurtosis across all NEON domains (results for NCA regions are reported in Figure S2 and Table S3).

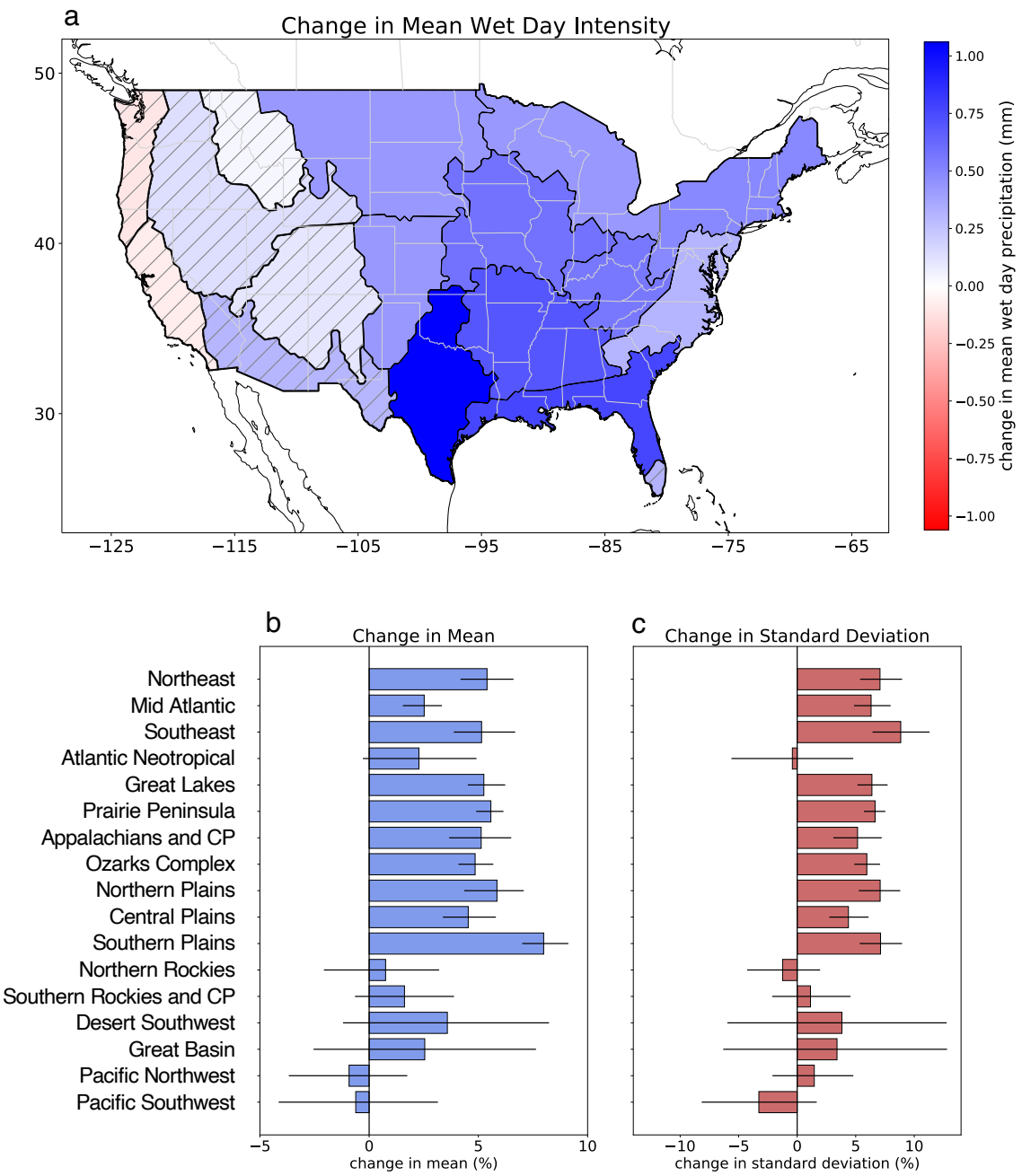

Figure 2: Changes in Wet Day Precipitation Intensity Between Early and Late Periods. (a) Map of changes in mean wet day precipitation intensity for NEON domains. Red-blue fill indicates change in precipitation intensity (mm/day) within domains (dark grey borders) on top of state boundaries (light

grey borders). Hatching denotes domains without statistically significant changes. (b) Percentage changes in mean wet day precipitation for NEON domains. Blue bars show percentage change of mean and horizontal black line shows 95% confidence interval. (c) Same as (b) but for standard deviation of wet day precipitation and with red bars.

In addition to changes in mean and standard deviation, we also quantify shifts in the underlying distributions across all precipitation intensities, allowing for a more nuanced characterization of observed distribution changes. Figure 3 illustrates smoothed observed shifts as determined by block bootstrapping. There is a broadly consistent shift from lower- to higher-intensity wet days across the central and eastern U.S. (blue filled regions, Figure 3). These changes are determined for five percentile increments and a demonstration of the calculations for two bootstrap iterations is available in supporting information (Figure S3). We characterize absolute differences in wet day intensities in Figures S3c-d, along with relative differences in Figures S3e-f. For example, in Figure S3c, we demonstrate that in this iteration, the Great Lakes domain has experienced a robust shift from lower to higher precipitation intensities across the full distribution of intensities, which becomes clearer when relativized against the initial early period frequencies in the early period (Figure S3e). To illustrate, the likelihood of a 95-100th percentile event has increased by roughly 15% in the Great Lakes in the later period of observation (Figure S3e-f).

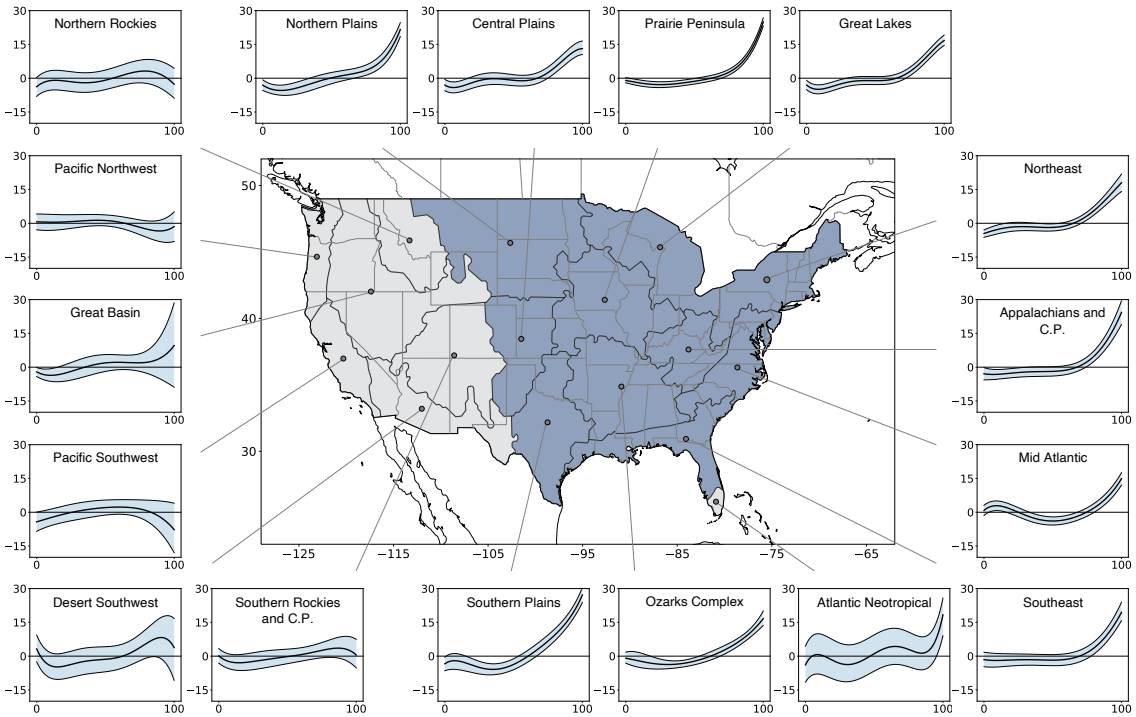

Figure 3: Smoothed Relativized Frequency Change for Each Domain. (map) The United States with NEON domain boundaries (thick dark grey) and state borders (thin light grey). Blue fill denotes the cluster of central and eastern domains with a predominantly consistent significant change in frequency across intensities. Conversely, grey fill denotes the cluster of western domains with inconsistent or non-significant changes in frequency across intensities. (domain subplots) Smoothed change in relative frequency of wet day intensity for each domain. Relative frequency change is determined at five percentile increments before smoothing is performed across three increments; a fifth-order polynomial is fit to the subsequent smoothed data. This is shown for the median (thick black) and 90% confidence bounds (thin black line and light blue shading) as determined by block bootstrapping. See Figure S3 for demonstration of underlying calculations and Figure S4 for raw (non-smoothed) results.

The shift from lower- to higher-intensity events is largely consistent in the central and eastern U.S., with lower-intensity events decreasing in relative frequency for all but one domain (Atlantic Neotropical; blue filled regions, Figure 3) and a broadly consistent increase of ~15% in the relative frequency of highest intensity events. However, while higher-intensity events generally increase for all central and eastern domains and intensities, this change is not uniform. For example, we observe no increase in the Atlantic Neotropical domain and a decrease in moderate intensity events in the Mid Atlantic domain. Similar to the mixed responses in mean wet day precipitation changes, changes across distribution frequencies vary between domains in the western U.S. (see grey filled regions, Figure 3), though they are generally not statistically significant. For example, shifts within the Southern Rockies and Colorado Plateau, Desert Southwest, and Great Basin domains show similar, but muted, low- to high-intensity shifts like the eastern U.S. This change is juxtaposed against nearby regions such as the Pacific Northwest, where a decrease in the highest-intensity events is observed. We also find similar spatial patterns in intensity shift for extreme events (99-100th percentile), though the increase in relative frequency of events in the eastern U.S. are higher (~20%). Additionally, we include findings for NCA regions and 99th-plus percentile events in Supporting Information (Figures S5-S10).

4. Discussion

Here, we examine the full extent of wet day precipitation intensity distributions and reveal statistically robust changes throughout the United States. Broadly, our analysis reveals an increase in mean wet day precipitation in the central and eastern U.S. from 1951-1980 to 1991-2020 driven by a shift from lower- to higher-intensity wet day events. Changes in the mean and standard deviation of wet day precipitation and underlying wet day intensity distribution shifts are mixed and do not reach statistical significance in the western U.S. Despite these western U.S. results, there is a statistically significant change in underlying wet day precipitation intensity distributions for all seventeen domains analyzed.

Though existing observation-based literature largely focuses on heavy-to-extreme precipitation or arbitrary light or moderate thresholds, our findings largely complement earlier findings, such as an east-west division of changes in extreme precipitation (Easterling et al., 2017). The relative increases in moderate and heavy precipitation we observe in the eastern U.S. mirror well-established increases in precipitation extremes, as well as annual precipitation, previously found over central and northeastern portions of the country (e.g., Groisman et al., 2012). We highlight the strong consistency in the shift in precipitation intensities across the distributions in this area (Figure 2) as well as the rising mean (~4.5-5.7%) and standard deviation (~4.4-8.7%) of wet day precipitation. While not a perfect parallel, the consistent shift from lower to higher intensity events in the central and eastern U.S. generally agrees with model-based findings from Dai et al. (2017), who examined U.S. precipitation intensities using historical and end-of-the-21st century RCP8.5 projections as boundary conditions in convection-permitting simulations (Liu et al., 2017). Dai et al. found robust increases in precipitation intensity across the U.S., a pattern we observe only in the central and eastern U.S. The mixed

pattern of results we find for the western U.S. mirrors earlier observation-based results (Contractor et al., 2021; Higgins and Kousky, 2013; Rosenberg et al., 2010). Our analysis furthers this earlier work by using a large number of in situ measurements instead of limited stations or gridded products. In addition, we note that Dai et al., along with other modeling studies we reference hereafter, use the RCP8.5 high emissions scenario, a pathway viewed as unlikely given societal trends (Hausfather and Peters, 2020). Despite its unlikelihood, we find it notable that the patterns of observed precipitation change presented here parallel RCP8.5-forced projections.

While our work does not assess the drivers of observed precipitation changes, we compare our findings with modeling studies to provide mechanistic context, though analogs to our retrospective, observation-based methodology and time periods of analysis are indirect. Pfahl et al. (2017) combine historical (1950-2005) CMIP5 output with RCP8.5 emissions scenario (2006-2100) simulations to project a positive scaling of moisture content (thermodynamic factor) with temperature throughout the U.S., with enhanced vertical motion (dynamic factor) over the western and far eastern U.S. (see Figure S5 in Pfahl et al., 2017). Similarly, Zhang et al. (2021) compare historical HadGEM3 output (1900-1959) to end-of-century RCP8.5 emissions scenario projections (2040-2099) to find that increases in synoptic-scale precipitation variability over the U.S. are driven by thermodynamic and non-linear mechanisms but dampened by dynamic drivers (see Figure 6 in Zhang et al., 2021). Broadly, these findings demonstrate a consistent increase in precipitation and synoptic-scale precipitation variability over the U.S. driven by thermodynamic influences and a mixture of dynamical influences. While some of the scaling unveiled in these previously published model analyses mirror our findings, such as an overlap

between thermodynamic drivers and the increases in precipitation intensity we observe across the eastern half of the U.S., further work is necessary to explain the mechanisms driving the changes in observed wet day precipitation intensity that we find. However, the overall pattern we identify – of a transition from lower- to higher-intensity events – mirrors findings from Pendergrass and Hartmann (2014b) for a modeled doubled-CO_2 world.

Although we examine precipitation trends during a time of increasing greenhouse gas concentrations, and find similarities with greenhouse gas-forced model projections, our analysis is insufficient to directly attribute observed changes to ongoing anthropogenic climate change. Such an analysis would require use of a robust attribution methodology (e.g., Hegerl et al., 1996). In addition, while considering our results, it is important to bear in mind that our analysis focuses on changes in *wet day* precipitation intensity, and therefore does not consider underlying changes in precipitation frequency. This distinction is important for considering the impacts of these findings in the scope of total annual precipitation, for example. In regions where precipitation intensity has increased but precipitation frequency has decreased by an offsetting or greater amount, changes to total annual precipitation may appear to run counter to the changes we describe here (e.g., Markonis et al., 2019). It is also important to consider potential limitations of this study, beginning with the underlying assumption that NEON domains are internally consistent. While NEON domains are empirically designed to possess internally homogeneous climates, there exists some measure of variability within domains, particularly within the varied topography of mountainous domains (e.g., Southern Rockies and Colorado Plateau). Additionally, inconsistent station availability may impact domain-level findings and variable station density may inadvertently weight domain-level results.

5. Conclusion

We use curated daily *in situ* precipitation measurements from the GHCN to examine regional trends in wet day precipitation distributions from 1951-1980 to 1991-2020. We reveal significant changes in wet day intensity distributions for all seventeen NEON domains in the contiguous United States. These nearly ubiquitous changes are driven by a general shift from lower to higher intensity wet day precipitation totals particularly within the central and eastern U.S. and are largely manifested as increases in the mean and standard deviation of wet day precipitation intensity, though findings are mixed in the western U.S. Our findings can help inform an understanding of how natural hazards and associated risks have changed over time. Additionally, these results can be compared with climate model output to examine the ability of climate models to accurately reproduce observed patterns of precipitation change.

Acknowledgements

We thank editor Alessandra Giannini at Geophysical Research Letters, along with Yiannis Moustakis and two anonymous reviewers, for their careful consideration of this work and insightful comments. We acknowledge and thank the National Centers for Environmental Information for the use of their publicly available Global Historical Climatology Network Daily dataset. We also express our gratitude for the Ubben Program for Carbon and Climate Science at Northwestern University for supporting and facilitating this work through a postdoctoral

fellowship to Ryan D. Harp. Finally, this research was supported in part through the computational resources and staff contributions provided for the Quest high performance computing facility at Northwestern University, which is jointly supported by the Office of the Provost, the Office for Research, and Northwestern University Information Technology.

Open Research and Availability Statement

Global Historical Climatology Network Daily data is publicly available through the National Centers for Environmental Information at https://www.ncei.noaa.gov/products/land-based-station/global-historical-climatology-network-daily. Code developed by the authors to conduct the analysis and produce the figures within this study is available at https://github.com/ryandharp/Observed_Changes_in_Daily_Precipitation_Intensity_in_the_United_States. This code will be archived on Zenodo upon completion of the peer review process, at which time the finalized link to archive, DOI, and data citation will be added to this statement.

411 **References**

412

413 Alexander, L. V., Bador, M., Roca, R., Contractor, S., Donat, M. G., & Nguyen, P. L. (2020).
414 Intercomparison of annual precipitation indices and extremes over global land areas from in
415 situ, space-based and reanalysis products. Environmental Research Letters, 15(5), 055002.

416

417 Alexander, L. V., Zhang, X., Peterson, T. C., Caesar, J., Gleason, B., Klein Tank, A. M. G.,
418 Haylock, M., Collins, D., Trewin, B., Rahimzadeh, F., Tagipour, A., Rupa Kumar, K., Revadekar,
419 J., Griffiths, G., Vincent, L., Stephenson, D. B., Burn, J., Aguilar, E., Brunet, M., Taylor, M., New,
420 M., Zhai, P., Rusticucci, M., & Vazquez-Aguirre, J. L. (2006). Global observed changes in daily
421 climate extremes of temperature and precipitation. Journal of Geophysical Research:
422 Atmospheres, 111(D5).

423

424 Asadieh, B., & Krakauer, N. Y. (2015). Global trends in extreme precipitation: climate models
425 versus observations. Hydrology and Earth System Sciences, 19(2), 877-891.

426

427 Bador, M., Donat, M. G., Geoffroy, O., & Alexander, L. V. (2018). Assessing the robustness of
428 future extreme precipitation intensification in the CMIP5 ensemble. Journal of Climate, 31(16),
429 6505-6525.

430

431 Berg, P., & Haerter, J. O. (2013). Unexpected increase in precipitation intensity with
432 temperature—A result of mixing of precipitation types?. Atmospheric Research, 119, 56-61.

Berg, P., Moseley, C., & Haerter, J. O. (2013). Strong increase in convective precipitation in response to higher temperatures. Nature Geoscience, 6(3), 181-185.

Caloiero, T., Caloiero, P., & Frustaci, F. (2018). Long-term precipitation trend analysis in Europe and in the Mediterranean basin. Water Environ. J. 32 (3), 433–445.

Cannon, S. H., Gartner, J. E., Wilson, R. C., Bowers, J. C., & Laber, J. L. (2008). Storm rainfall conditions for floods and debris flows from recently burned areas in southwestern Colorado and southern California. Geomorphology, 96(3-4), 250-269.

Cannon, A. J., & Innocenti, S. (2019). Projected intensification of sub-daily and daily rainfall extremes in convection-permitting climate model simulations over North America: implications for future intensity–duration–frequency curves. Natural Hazards and Earth System Sciences, 19(2), 421-440.

Chakravarti, I. M., Laha, R. G., & Roy, J. (1967). Handbook of methods of applied statistics. Wiley Series in Probability and Mathematical Statistics (USA) eng.

Chou, C., Chen, C. A., Tan, P. H., & Chen, K. T. (2012). Mechanisms for global warming impacts on precipitation frequency and intensity. Journal of Climate, 25(9), 3291-3306.

Contractor, S., Donat, M. G., & Alexander, L. V. (2021). Changes in observed daily precipitation over global land areas since 1950. Journal of Climate, 34(1), 3-19.

Cook, L. M., VanBriesen, J. M., & Samaras, C. (2019). Using rainfall measures to evaluate hydrologic performance of green infrastructure systems under climate change. Sustainable and Resilient Infrastructure, 6(3-4), 156-180.

Dai, A., Rasmussen, R. M., Liu, C., Ikeda, K., & Prein, A. F. (2017). A new mechanism for warm-season precipitation response to global warming based on convection-permitting simulations. Climate Dynamics, 55(1), 343-368.

Dinis, P. A., Huvi, J., Cabral Pinto, M., & Carvalho, J. (2021). Disastrous Flash Floods Triggered by Moderate to Minor Rainfall Events. Recent Cases in Coastal Benguela (Angola). Hydrology, 8(2), 73.

Donat, M. G., Lowry, A. L., Alexander, L. V., O'Gorman, P. A., & Maher, N. (2016). More extreme precipitation in the world's dry and wet regions. Nature Climate Change, 6(5), 508-513.

Douville, H., Raghavan, K., Renwick, J., Allan, R. P., Arias, P. A., Barlow, M., Cerezo-Mota, R., Cherchi, A., Gan, T. Y., Gergis, J., Jiang, D., Khan, A., Pokam Mba, W., Rosenfeld, D., Tierney, J., & Zolina, O. (2021): Water Cycle Changes. In Climate Change 2021: The Physical Science Basis.

476 Contribution of Working Group I to the Sixth Assessment Report of the Intergovernmental
477 Panel on Climate Change.
478
479 Durre, I., Menne, M. J., Gleason, B. E., Houston, T. G., & Vose, R. S. (2010). Comprehensive
480 automated quality assurance of daily surface observations. Journal of Applied Meteorology and
481 Climatology, 49(8), 1615-1633.
482
483 Easterling, D. R., Kunkel, K. E., Arnold, J. R., Knutson, T., LeGrande, A. N., Leung, L. R., Vose,
484 R. S., Waliser, D. E., & Wehner, M. F. (2017): Precipitation change in the United States. In:
485 Climate Science Special Report: Fourth National Climate Assessment, Volume I.
486
487 Endo, H., & Kitoh, A. (2014). Thermodynamic and dynamic effects on regional monsoon rainfall
488 changes in a warmer climate. Geophysical Research Letters, 41(5), 1704-1711.
489
490 Fischer, E. M., Beyerle, U., & Knutti, R. (2013). Robust spatially aggregated projections of
491 climate extremes. Nature Climate Change, 3(12), 1033-1038.
492
493 Fischer, E. M., & Knutti, R. (2014). Detection of spatially aggregated changes in temperature and
494 precipitation extremes. Geophysical Research Letters, 41(2), 547-554.
495
496 Fischer, E. M., & Knutti, R. (2016). Observed heavy precipitation increase confirms theory and
497 early models. Nature Climate Change, 6(11), 986-991.

Giorgi, F., Raffaele, F., & Coppola, E. (2019). The response of precipitation characteristics to global warming from climate projections. Earth System Dynamics, 10(1), 73-89.

Goble, P. E., Doesken, N. J., Durre, I., Schumacher, R. S., Stewart, A., & Turner, J. (2020). Strength in Numbers: Daily Precipitation Extremes over CONUS. Bulletin of the American Meteorological Society, 101(8), 679-682.

Goodwell, A. E., & Kumar, P. (2019). A changing climatology of precipitation persistence across the United States using information-based measures. Journal of Hydrometeorology, 20(8), 1649-1666.

Groisman, P. Y., Knight, R. W., Easterling, D. R., Karl, T. R., Hegerl, G. C., & Razuvaev, V. N. (2005). Trends in intense precipitation in the climate record. Journal of climate, 18(9), 1326-1350.

Groisman, P. Y., Knight, R. W., & Karl, T. R. (2001). Heavy precipitation and high streamflow in the contiguous United States: Trends in the twentieth century. Bulletin of the American Meteorological Society, 82(2), 219-246.

Groisman, P. Y., Knight, R. W., & Karl, T. R. (2012). Changes in intense precipitation over the central United States. Journal of Hydrometeorology, 13(1), 47-66.

Guerreiro, S. B., Fowler, H. J., Barbero, R., Westra, S., Lenderink, G., Blenkinsop, S., Lewis, E., & Li, X. F. (2018). Detection of continental-scale intensification of hourly rainfall extremes. Nature Climate Change, 8(9), 803-807.

Guilbert, J., Betts, A. K., Rizzo, D. M., Beckage, B., & Bomblies, A. (2015). Characterization of increased persistence and intensity of precipitation in the northeastern United States. Geophysical Research Letters, 42(6), 1888-1893.

Hausfather, Z., & Peters, G. P. (2020). Emissions–the 'business as usual' story is misleading. Nature, 577, 618-620.

Hegerl, G. C., von Storch, H., Hasselmann, K., Santer, B. D., Cubasch, U., & Jones, P. D. (1996). Detecting greenhouse-gas-induced climate change with an optimal fingerprint method. Journal of Climate, 9(10), 2281-2306.

Held, I. M., & Soden, B. J. (2006). Robust responses of the hydrological cycle to global warming. Journal of climate, 19(21), 5686-5699.

Hennessy, K. J., Gregory, J. M., & Mitchell, J. F. B. (1997). Changes in daily precipitation under enhanced greenhouse conditions. Climate Dynamics, 13(9), 667-680.

541 Higgins, R. W., & Kousky, V. E. (2013). Changes in observed daily precipitation over the United
542 States between 1950–79 and 1980–2009. Journal of Hydrometeorology, 14(1), 105-121.
543
544 Ivancic, T. J., & Shaw, S. B. (2016). A US-based analysis of the ability of the Clausius-Clapeyron
545 relationship to explain changes in extreme rainfall with changing temperature. Journal of
546 Geophysical Research: Atmospheres, 121(7), 3066-3078.
547
548 Kahraman, A., Kendon, E. J., Chan, S. C., & Fowler, H. J. (2021). Quasi-stationary intense
549 rainstorms spread across Europe under climate change. Geophysical Research Letters, 48(13),
550 e2020GL092361.
551
552 Karl, T. R., & Knight, R. W. (1998). Secular trends of precipitation amount, frequency, and
553 intensity in the United States. Bulletin of the American Meteorological Society, 79(2), 231-242.
554
555 Keller, M., Schimel, D. S., Hargrove, W. W., & Hoffman, F. M. (2008). A continental strategy for
556 the National Ecological Observatory Network. The Ecological Society of America: 282-284.
557
558 Kunkel, K. E., Karl, T. R., Brooks, H., Kossin, J., Lawrimore, J. H., Arndt, D., Bosart, L.,
559 Changnon, D., Cutter, S. L., Doesken, N., Emanuel, K., Groisman, P. Y., Katz, R. W., Knutson, T.,
560 O'Brien, J., Paciorek, C. J., Peterson, T. C., Redmond, K., Robinson, D., Trapp, J., Vose, R.,
561 Weaver, S., Wehner, M., Wolter, K., & Wuebbles, D. (2013). Monitoring and understanding

562 trends in extreme storms: State of knowledge. Bulletin of the American Meteorological Society,
563 94(4), 499-514.
564
565 Lehmann, J., Coumou, D., & Frieler, K. (2015). Increased record-breaking precipitation events
566 under global warming. Climatic Change, 132(4), 501-515.
567
568 Lenderink, G., & Van Meijgaard, E. (2008). Increase in hourly precipitation extremes beyond
569 expectations from temperature changes. Nature Geoscience, 1(8), 511-514.
570
571 Liu, C., Ikeda, K., Rasmussen, R., Barlage, M., Newman, A. J., Prein, A. F., Chen, F., Chen, L.,
572 Clark, M., Dai, A., Dudhia, J., Eidhammer, T., Gochis, D., Gutmann, E., Kurkute, S., Li, Y.,
573 Thompson, G., & Yates, D. (2017). Continental-scale convection-permitting modeling of the
574 current and future climate of North America. Climate Dynamics, 49(1), 71-95.
575
576 Markonis, Y., Papalexiou, S. M., Martinkova, M., & Hanel, M. (2019). Assessment of water cycle
577 intensification over land using a multisource global gridded precipitation dataset. Journal of
578 Geophysical Research: Atmospheres, 124(21), 11175-11187.
579
580 Menne, M. J., Durre, I., Vose, R. S., Gleason, B. E., & Houston, T. G. (2012). An overview of the
581 global historical climatology network-daily database. Journal of atmospheric and oceanic
582 technology, 29(7), 897-910.
583

584 Min, S. K., Zhang, X., Zwiers, F. W., & Hegerl, G. C. (2011). Human contribution to more-intense
585 precipitation extremes. Nature, 470(7334), 378-381.
586
587 Moustakis, Y., Onof, C. J., & Paschalis, A. (2020). Atmospheric convection, dynamics and
588 topography shape the scaling pattern of hourly rainfall extremes with temperature globally.
589 Communications Earth & Environment, 1(1), 1-9.
590
591 Moustakis, Y., Papalexiou, S. M., Onof, C. J., & Paschalis, A. (2021). Seasonality, intensity, and
592 duration of rainfall extremes change in a warmer climate. Earth's Future, 9(3), e2020EF001824.
593
594 Myhre, G., Alterskjær, K., Stjern, C. W., Hodnebrog, Ø., Marelle, L., Samset, B. H., Sillmann, J.,
595 Schaller, N., Fischer, E., Schulz, M., & Stohl, A. (2019). Frequency of extreme precipitation
596 increases extensively with event rareness under global warming. Scientific reports, 9(1), 1-10.
597
598 National Ecological Observatory Network (n.d.). Spatial and Temporal Design. NEON Science.
599 https://www.neonscience.org/about/overview/design
600
601 O'Gorman, P. A. (2015). Precipitation extremes under climate change. Current climate change
602 reports, 1(2), 49-59.
603

Pal, I., Anderson, B. T., Salvucci, G. D., & Gianotti, D. J. (2013). Shifting seasonality and increasing frequency of precipitation in wet and dry seasons across the US. Geophysical Research Letters, 40(15), 4030-4035.

Pendergrass, A. G., & Hartmann, D. L. (2014a). The atmospheric energy constraint on global-mean precipitation change. Journal of climate, 27(2), 757-768.

Pendergrass, A. G., & Hartmann, D. L. (2014b). Changes in the distribution of rain frequency and intensity in response to global warming. Journal of Climate, 27(22), 8372-8383.

Pfahl, S., O'Gorman, P. A., & Fischer, E. M. (2017). Understanding the regional pattern of projected future changes in extreme precipitation. Nature Climate Change, 7(6), 423-427.

Polade, S. D., Pierce, D. W., Cayan, D. R., Gershunov, A., & Dettinger, M. D. (2014). The key role of dry days in changing regional climate and precipitation regimes. Scientific reports, 4(1), 1-8.

Prein, A. F., Rasmussen, R. M., Ikeda, K., Liu, C., Clark, M. P., & Holland, G. J. (2017). The future intensification of hourly precipitation extremes. Nature Climate Change, 7(1), 48-52.

Pryor, S. C., Howe, J. A., & Kunkel, K. E. (2008). How spatially coherent and statistically robust are temporal changes in extreme precipitation in the contiguous USA?. International Journal of Climatology: A Journal of the Royal Meteorological Society, 29(1), 31-45.

Risser, M. D., & Wehner, M. F. (2017). Attributable human-induced changes in the likelihood and magnitude of the observed extreme precipitation during Hurricane Harvey. Geophysical Research Letters, 44(24), 12-457.

Roque-Malo, S., & Kumar, P. (2017). Patterns of change in high frequency precipitation variability over North America. Scientific reports, 7(1), 1-12.

Rosenberg, E. A., Keys, P. W., Booth, D. B., Hartley, D., Burkey, J., Steinemann, A. C., & Lettenmaier, D. P. (2010). Precipitation extremes and the impacts of climate change on stormwater infrastructure in Washington State. Climatic change, 102(1), 319-349.

Schimel, D. (2011). The era of continental-scale ecology. Frontiers in Ecology and the Environment, 9(6), 311-311.

Seneviratne, S.I., Zhang, X., Adnan, M., Badi, W., Dereczynski, C., Di Luca, A., Ghosh, S., Iskandar, I., Kossin, J., Lewis, S., Otto, F., Pinto, I., Satoh, M., Vicente-Serrano, S. M., Wehner, M., & Zhou, B. (2021): Weather and Climate Extreme Events in a Changing Climate. In Climate Change 2021: The Physical Science Basis. Contribution of Working Group I to the Sixth Assessment Report of the Intergovernmental Panel on Climate Change.

Shortridge, J. (2019). Observed trends in daily rainfall variability result in more severe climate change impacts to agriculture. Climatic Change, 157(3), 429-444.

Stephens, M. A. (1974). EDF statistics for goodness of fit and some comparisons. Journal of the American Statistical Association, 69(347), 730-737.

Sun, Q., Zhang, X., Zwiers, F., Westra, S., & Alexander, L. V. (2021). A global, continental, and regional analysis of changes in extreme precipitation. Journal of Climate, 34(1), 243-258.

Swain, D. L., Horton, D. E., Singh, D., & Diffenbaugh, N. S. (2016). Trends in atmospheric patterns conducive to seasonal precipitation and temperature extremes in California. Science Advances, 2(4), e1501344.

Toreti, A., Naveau, P., Zampieri, M., Schindler, A., Scoccimarro, E., Xoplaki, E., Dijkstra, H. A., Gualdi, S., & Luterbacher, J. (2013). Projections of global changes in precipitation extremes from Coupled Model Intercomparison Project Phase 5 models. Geophysical Research Letters, 40(18), 4887-4892.

Trenberth, K. E., Dai, A., Rasmussen, R. M., & Parsons, D. B. (2003). The changing character of precipitation. Bulletin of the American Meteorological Society, 84(9), 1205-1218.

668 Villarini, G., Smith, J. A., & Vecchi, G. A. (2013). Changing frequency of heavy rainfall over the
669 central United States. Journal of Climate, 26(1), 351-357.
670
671 Wentz, F. J., Ricciardulli, L., Hilburn, K., & Mears, C. (2007). How much more rain will global
672 warming bring?. Science, 317(5835), 233-235.
673
674 Westra, S. HJ Fowler, JP Evans, LV Alexander, P. Berg, F. Johnson, EJ Kendon, G. Lenderink,
675 and NM Roberts, 2014: Future changes to the intensity and frequency of short-duration extreme
676 rainfall. Reviews of Geophysics, 52, 522-555.
677
678 Wood, R. R., & Ludwig, R. (2020). Analyzing internal variability and forced response of
679 subdaily and daily extreme precipitation over Europe. Geophysical Research Letters, 47(17),
680 e2020GL089300.
681
682 Wood, R. R., Lehner, F., Pendergrass, A. G., & Schlunegger, S. (2021). Changes in precipitation
683 variability across time scales in multiple global climate model large ensembles. Environmental
684 Research Letters, 16(8), 084022.
685
686 World Meteorological Organization. (2017). WMO guidelines on the calculation of climate
687 normals.
688

689 Zhang, W., Furtado, K., Wu, P., Zhou, T., Chadwick, R., Marzin, C., Rostron, J., & Sexton, D.
690 (2021). Increasing precipitation variability on daily-to-multiyear time scales in a warmer world.
691 Science advances, 7(31), eabf8021.

Supporting Information for Observed Changes in Daily Precipitation Intensity in the United States

Ryan D. Harp, Daniel E. Horton

Resubmitted to Geophysical Research Letters

19 July, 2022

This document contains ten figures and three tables which are supplementary to the main text.

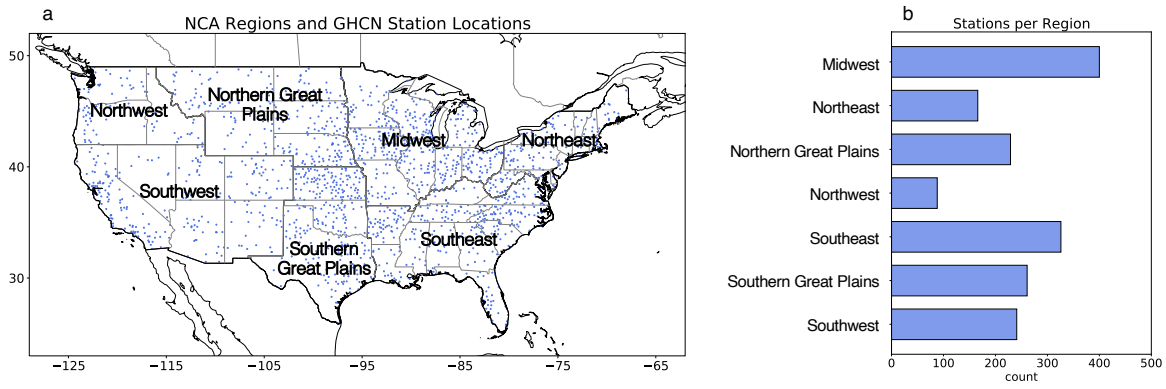

Figure S1*: Station Locations and NCA Region Station Counts. (a) Map of qualifying GHCN-D stations (blue dots) overlaid on the United States with U.S. National Climate Assessment (NCA) region boundaries in thick black and state borders in thin grey. (b) Histogram of the number of qualifying stations within each NCA region.*

Station ID	NEON Domain	NCA Region	Station-Block Years Removed	Outlier Values (mm)
USC00164700	Southeast	Southeast	1955-1956	764.5, 527.3, 791.5
USC00253185	Central Plains	Northern Great Plains	1963-1964	1524.5, 1778.8, 762.5, 1526.5, 2286, 1524.3, 1778, 2286, 1016, 1016, 2286, 508.5, 762, 763.8, 2286
USC00210287	Northern Plains	Midwest	1951-1952	290.8
USC00353604	Great Basin	Northwest	1951-1952	261.6
USW00003904	Southern Plains	Southern Great Plains	1971-1972	1016
USW00024284	Pacific Northwest	Northwest	1957-1958	283.7
USC00177479	Northeast	Northeast	1999-2000	584.2, 2006.6
USC00303346	Northeast	Northeast	1951-1952	1796.5
USC00200230	Great Lakes	Midwest	1953-1954	1286.3
USC00204090	Great Lakes	Midwest	1959-1960	2032.3
USC00335718	Appalachians and Cumberland Plateau	Midwest	1963-1964	457.2
USC00335747	Appalachians and Cumberland Plateau	Midwest	1965-1966	1017.3
USC00034562	Ozarks Complex	Southeast	1951-1952	1524.3
USC00422057	Southern Rockies and Colorado Plateau	Southwest	1973-1974	1524
USW00024057	Great Basin	Northern Great Plains	1967-1968	254.3

***Table S1**: List of Manually Identified Unverifiable Outliers. Outlying observations were compared against appropriate verified state and station records, etc. to determine validity; unverifiable records are listed here. Two-year station-blocks containing unverifiable records are removed from our analysis.*

	Mean	Standard Deviation	Median	Skew	Kurtosis
Northeast*	**5.4**	**7.0**	**5.7**	-0.3	-2.6
Mid Atlantic*	**2.5**	**6.3**	0.0	**17.6**	**11.1**
Southeast*	**5.2**	**8.8**	3.7	**11.3**	8.6
Atlantic Neotropical#	2.3	-0.4	7.0	-17.7	**-20.2**
Great Lakes*	**5.3**	**6.4**	6.3	-0.3	-0.4
Prairie Peninsula*	**5.6**	**6.7**	**5.2**	-0.2	0.5
Appalachians and Cumberland Plateau*	**5.1**	**5.2**	**4.5**	-5.1	-2.5
Ozarks Complex*	**4.9**	**6.0**	**3.5**	2.5	1.3
Northern Plains*	**5.8**	**7.1**	7.9	2.6	1.6
Central Plains*	**4.6**	**4.4**	5.7	-2.9	-1.1
Southern Plains*	**8.0**	**7.1**	**7.0**	-3.7	-1.2
Northern Rockies*	0.8	-1.3	0.0	-4.2	-1.2
Southern Rockies and Colorado Plateau*	1.7	1.2	**0.0**	4.9	7.5
Desert Southwest*	3.6	3.8	4.2	9.0	10.8
Great Basin*	2.5	3.4	0.0	**12.6**	**13.4**
Pacific Northwest*	-0.9	1.4	0.0	**10.4**	3.3
Pacific Southwest*	-0.6	-3.3	0.0	**-8.4**	**-5.3**
Tundra*	4.7	-1.4	7.1	**-14.0**	-4.8

Taiga	-0.2	-0.6	0.0	1.1	0.6
Pacific Tropical*	0.6	-3.3	0.0	-4.0	-1.2

***Table S2**: Percent Change in Wet Day Precipitation Intensity Distribution Moments. Bolded values denote statistical significance at the $p < 0.05$ level. Domains denoted with * observed statistically significant ($p < 0.05$) differences in early and late distributions from both the Kolmogorov-Smirnov and Anderson-Darling two-sample tests (# denotes statistically significant differences in Anderson-Darling two-sample test only).*

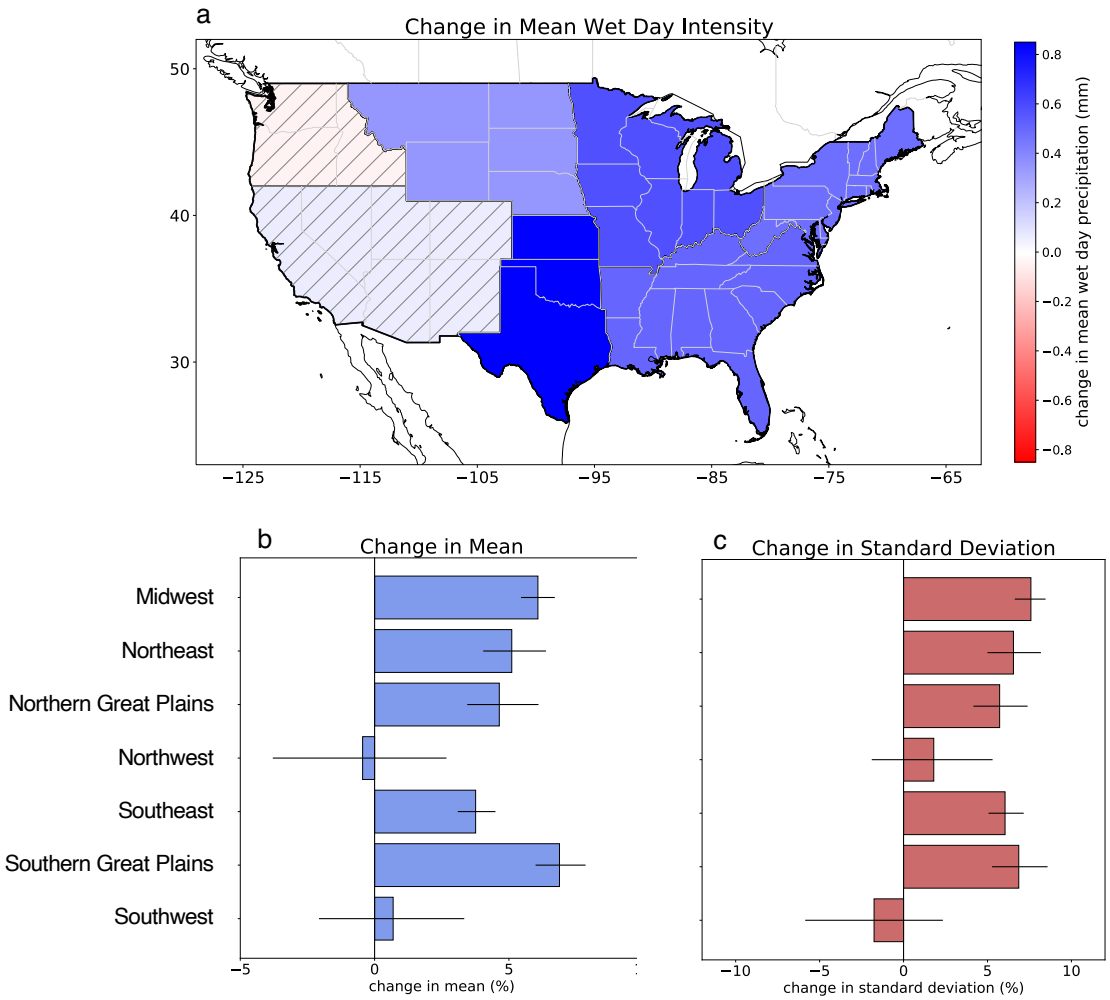

***Figure S2**: Changes in Wet Day Precipitation Intensity Between Early (1951-1980) and Late (1991-2020) Periods for NCA Regions. (a) Map of changes in mean wet day precipitation for NCA regions. Red-blue fill indicates change in precipitation intensity (mm/day) within domains (dark grey borders) on top of state boundaries (light grey borders). Hatching denotes domains without a statistically significant change in mean wet day precipitation intensity. (b) Percentage changes in mean wet day precipitation for NCA domains. Blue bars show percentage change of mean and horizontal black line shows 95% confidence interval. (c) Same as (b) but for standard deviation of wet day precipitation and with red bars.*

	Mean	Standard Deviation	Median	Skew	Kurtosis
Alaska	-0.1	-0.1	0.0	5.3	14.7
U.S. Caribbean	-	-	-	-	-
Hawaii and Pacific Islands#	-4.9	-7.9	0.0	2.5	11.4
Midwest*	**6.1**	**7.6**	0.0	0.9	4.5
Northeast*	**5.2**	**6.5**	**3.6**	1.3	0.3
Northern Great Plains*	**4.7**	**5.7**	4.9	2.2	7.4
Northwest*	-0.5	1.8	0.0	**10.3**	18.9
Southeast*	**3.8**	**6.1**	2.5	**6.8**	**18.9**
Southern Great Plains*	**6.9**	**6.9**	**7.6**	1.6	16.9
Southwest*	0.7	-1.7	4.3	-5.8	**-16.8**

Table S3*: Percent Change in Wet Day Precipitation Intensity Distribution Moments for NCA regions. Bolded values denote statistical significance at the $p < 0.05$ level. Domains denoted with * observed statistically significant ($p < 0.05$) differences in early and late distributions from both the Kolmogorov-Smirnov and Anderson-Darling two-sample tests (# denotes statistically significant differences in Anderson-Darling two-sample test only). Note that the U.S. Caribbean region does not contain any qualifying stations.*

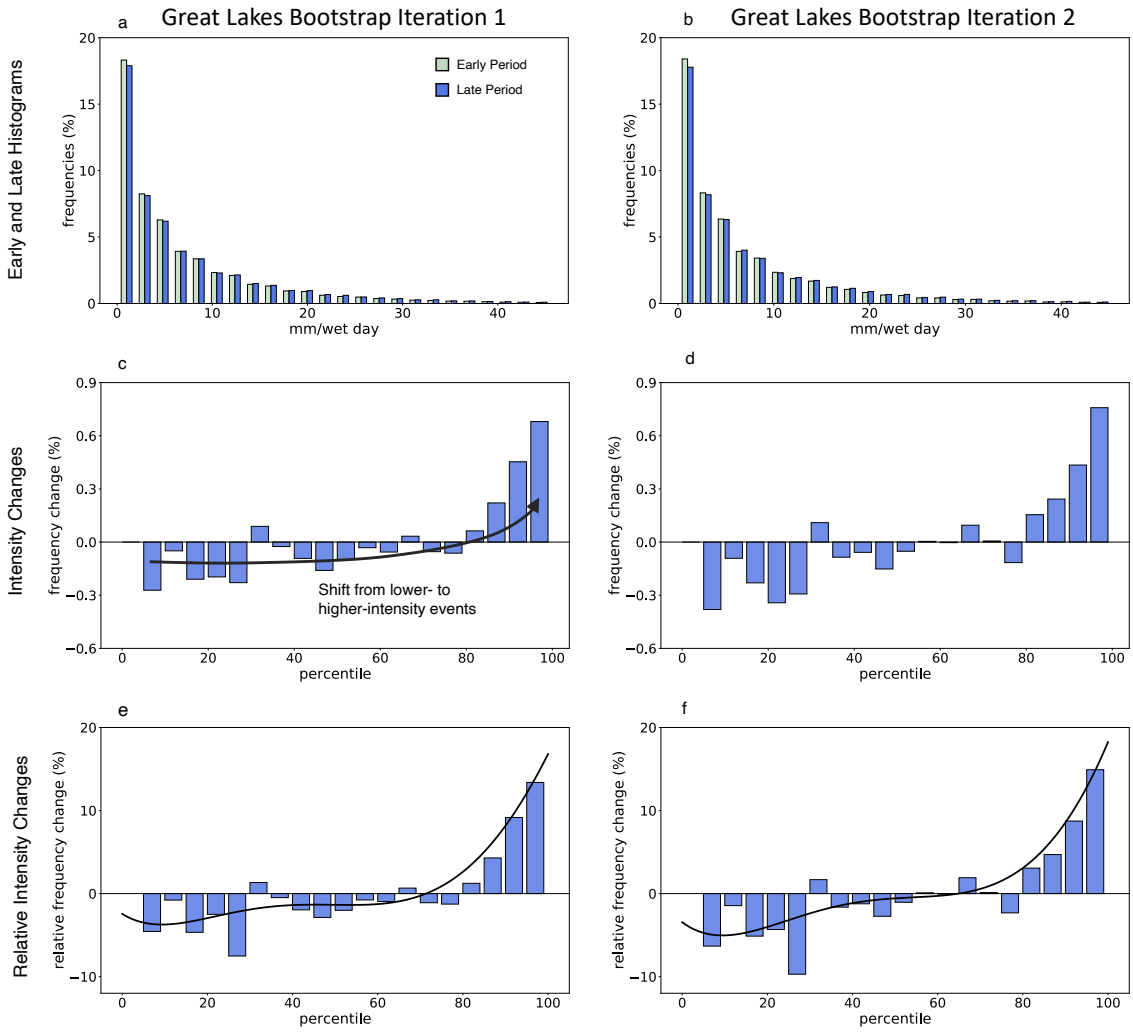

Figure S3*: Bootstrapped Change in Precipitation Intensity between Early and Late Periods. (a) Histograms of wet day precipitation intensity in the Great Lakes domain for the early (light green; 1951-1980) and late (dark blue; 1991-2020) period. Histogram values represent the percentage of all wet-day events within the binned intensity. (b) Absolute difference in wet day precipitation intensity frequency between the late and early periods for the Great Lakes NEON domain over five percentile increments. (c) Same as (b) but the change is normalized by the early period frequency. Thick black line represents a fifth-*

degree polynomial fit over a three bin smoothing. (d-f) Same as (a-c) but for a second iteration of the block bootstrapping methodology.

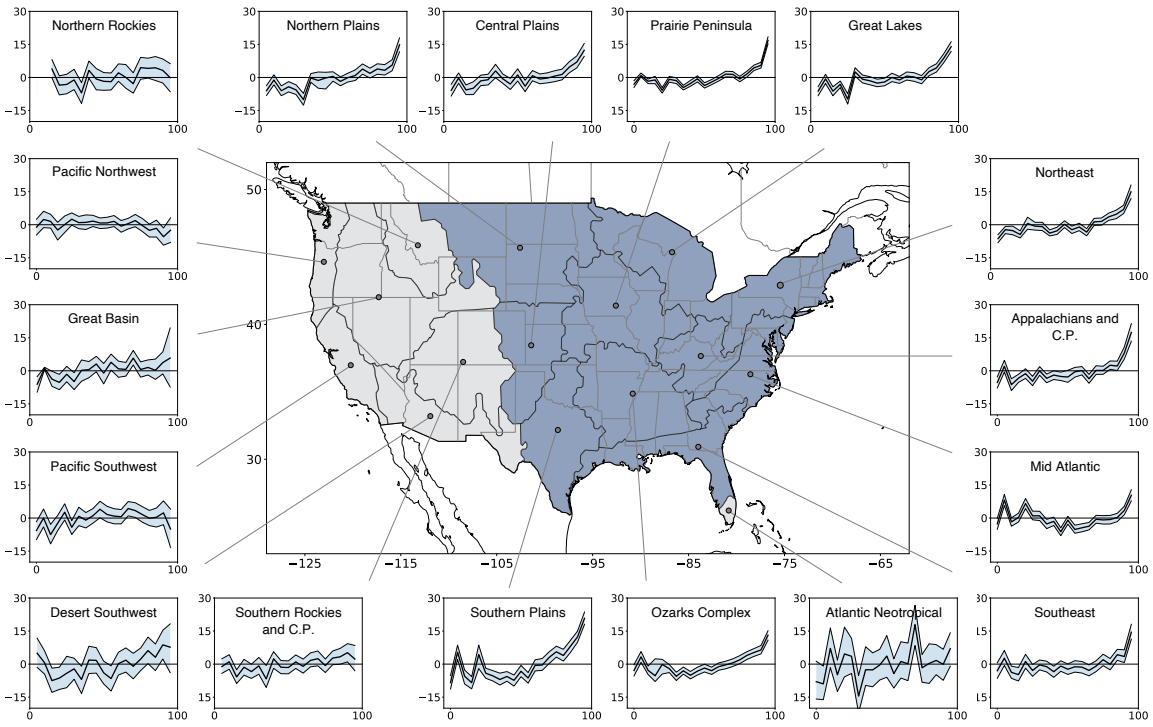

***Figure S4**: Raw Relativized Frequency Change for Each Domain. (map) The United States with NEON domain boundaries (thick dark grey) and state borders (thin light grey). Blue fill denotes the cluster of central and eastern domains with a predominantly consistent significant change in frequency across intensities. Conversely, grey fill denotes the cluster of western domains with inconsistent or non-significant changes in frequency across intensities. (domain subplots) Raw change in frequency of intensity for each domain across the 0th-100th percentile of wet day intensities at five percentile increments. This is illustrated for both the median (thick black) and 90% confidence bounds as determined by block bootstrapping (thin black line and light blue shading).*

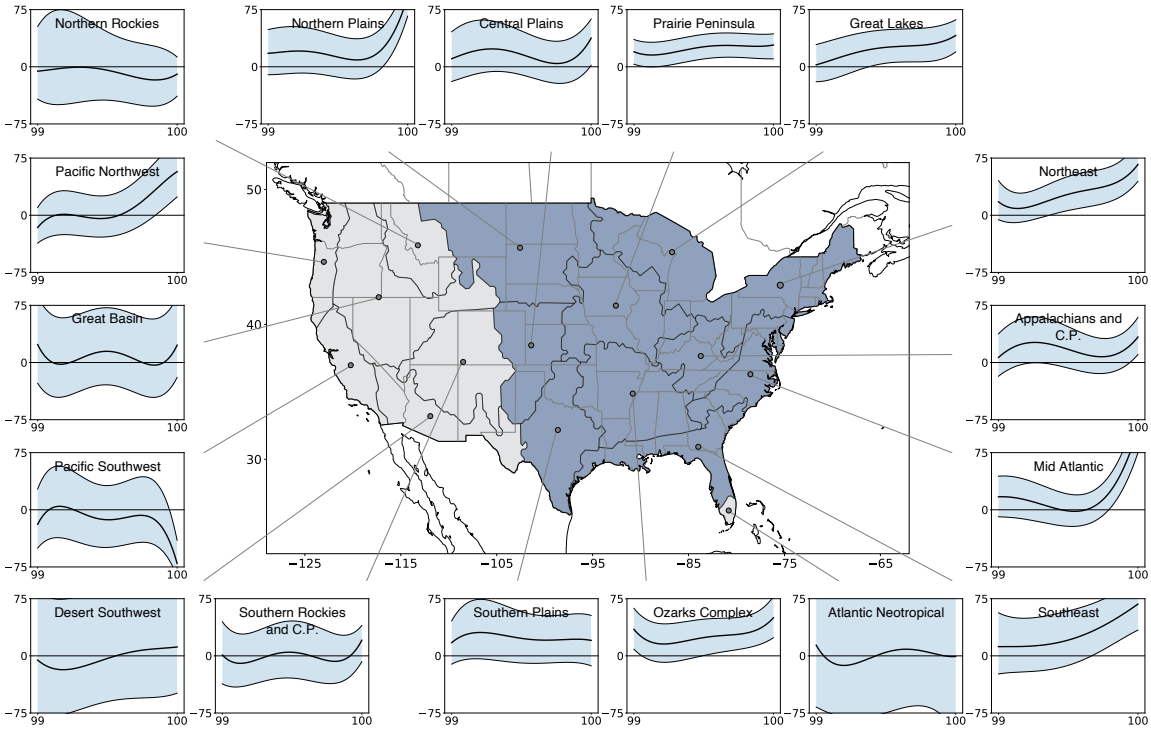

***Figure S5**: Smoothed Relativized Frequency Change for Each Domain for Extreme Precipitation. Same as Figure 3 but for 99th-100th percentile precipitation and 0.05 percentile increments.*

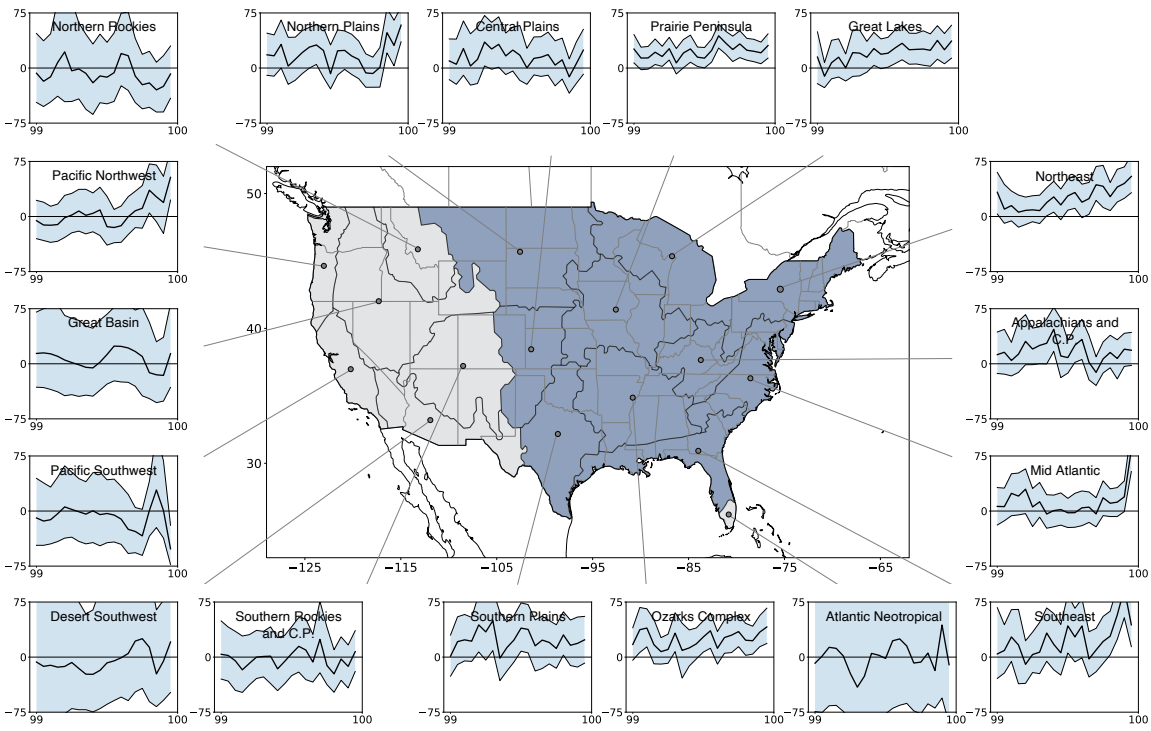

***Figure S6**: Raw Relativized Frequency Change for Each Domain for Extreme Precipitation. Same as Figure S4 but for 99th-100th percentile precipitation and 0.05 percentile increments.*

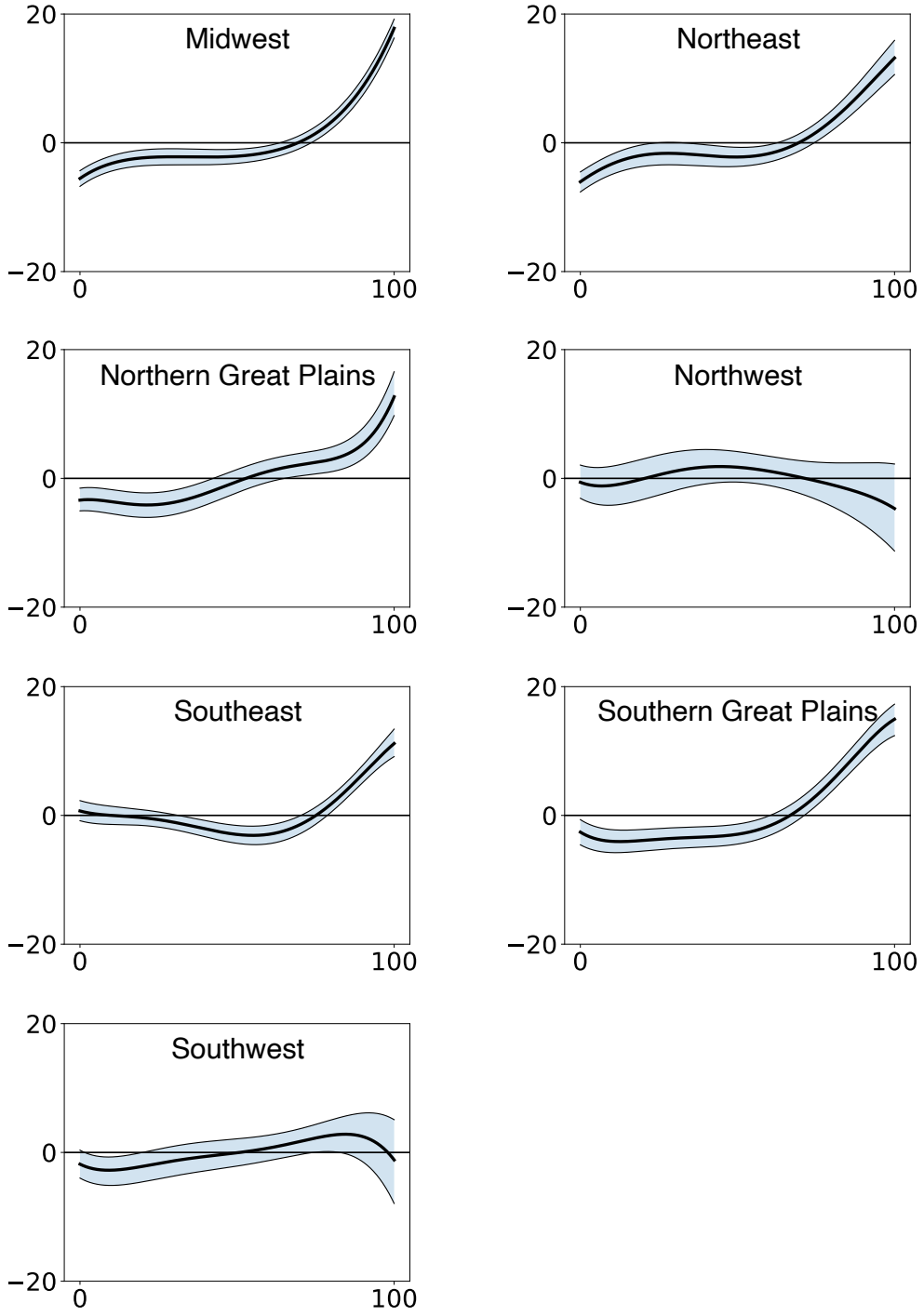

92

93 ***Figure S7****: Smoothed Relativized Frequency Change for Each NCA Region. Same as Figure 2 but for*

94 *NCA regions and without underlying map.*

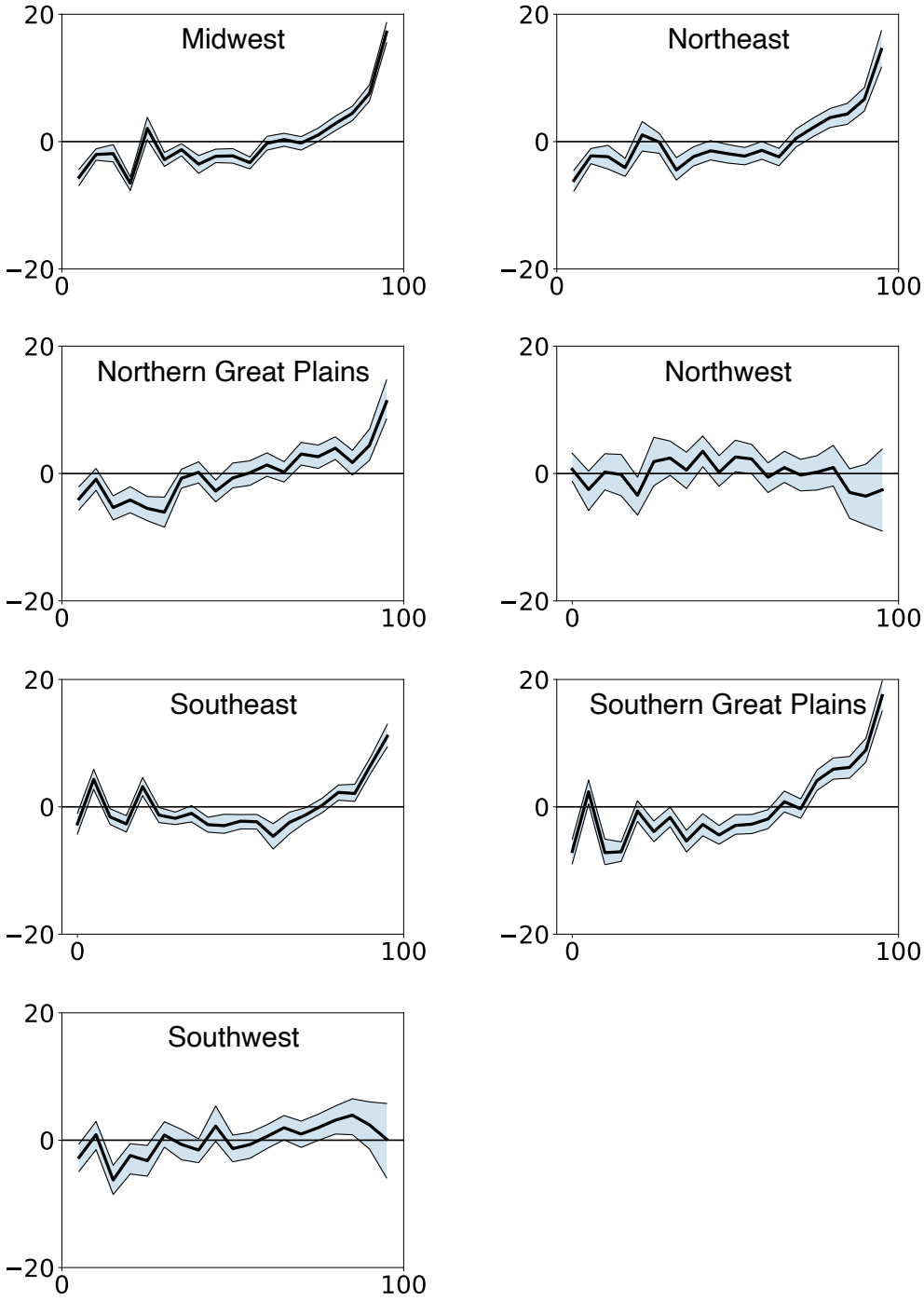

***Figure S8**: Raw Relativized Frequency Change for Each NCA Region. Same as Figure S4 but for NCA regions and without underlying map.*

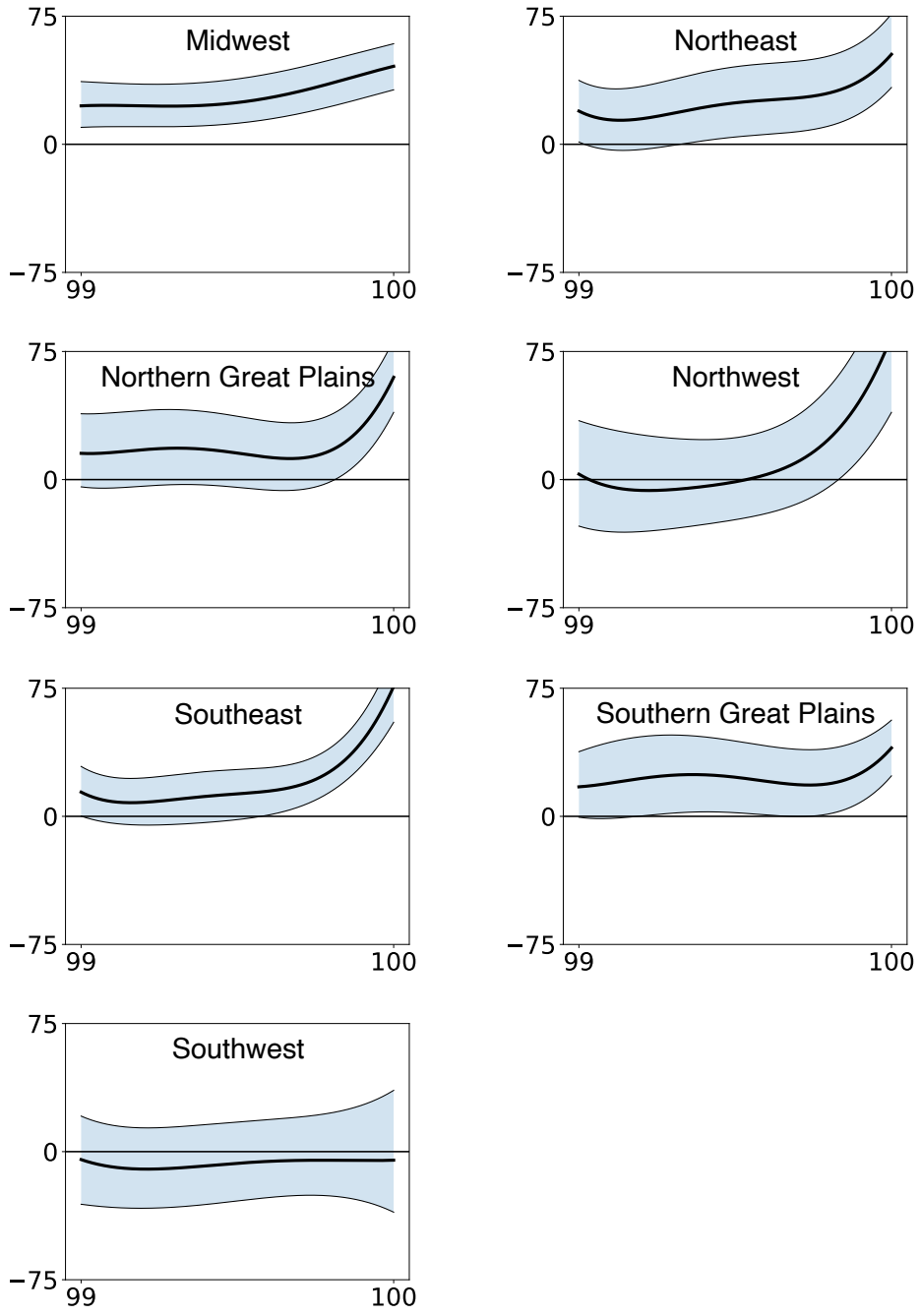

***Figure S9**: Smoothed Relativized Frequency Change for Each NCA Region for Extreme Precipitation.*

Same as Figure S5 but for NCA regions and without underlying map.

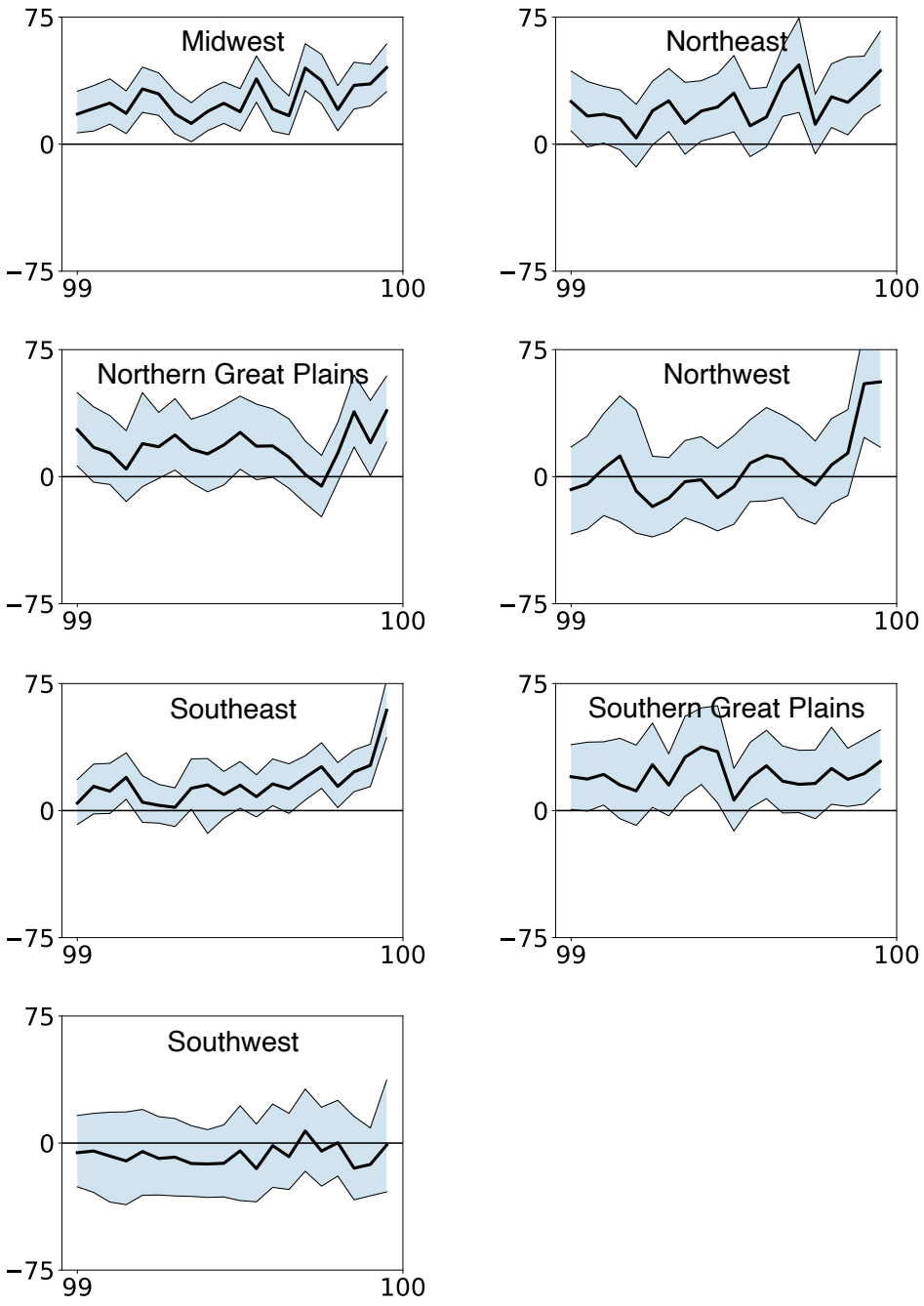

***Figure S10**: Raw Relativized Frequency Change for Each NCA Region for Extreme Precipitation. Same as Figure S6 but for NCA regions and without underlying map.*